



## CuO nanofluids: Particle-fluid interaction study using ultrasonic technique

Vijayta Gupta, Upasna Magotra, Sandarve, Amit Kumar Sharma and Meena Sharma\*

Department of Chemistry, University of Jammu (J&K), India

---

### ABSTRACT

*In the present investigation, ultrasonic studies of copper oxide (CuO) nanofluids are reported. Crystalline copper oxide nanoparticles are synthesized by co-precipitation method while the stable dispersions of nanosized CuO particles in ethylene glycol are prepared with the aid of sonication. The synthesized nanoparticles are characterized by X-ray powder diffractometry (XRD) to find the crystallinity and composition. Other characterization techniques such as SEM-EDX, TEM, and UV-visible are also provided to support the obtained results. Ultrasonic velocity, density and viscosity values are measured for different concentrations of CuO nanofluids at 25, 30 and 35°C. The acoustical parameters such as adiabatic compressibility ( $\beta_{ad}$ ), intermolecular free length ( $L_f$ ), relaxation time ( $\tau$ ), absorption coefficient ( $\alpha/f^2$ ), acoustic impedance (Z), Gibb's free energy ( $\Delta G$ ), free volume ( $V_f$ ), rao's constant ( $R_M$ ) and wada's constant (W) are calculated from the experimental data. The inter particle interactions of nanoparticles and the cluster formation are realized through the variations in ultrasonic parameters. The results demonstrate that the aggregation of CuO nanoparticles becomes predominant at higher concentrations.*

**Keywords:** ultrasonic, nanofluids, characterization, acoustical parameters, interactions

---

### INTRODUCTION

Nanofluid is a stable colloidal suspension of low volume fraction of nanoparticles dispersed in base fluids [1]. In general, the nanoparticles used in nanofluids are made of metals, oxides, carbides, or carbon nanotubes. Common base fluids used are water, ethylene glycol and oil. One interesting characteristic of nano fluids is that they have unusually high thermal conductivity, and hence they are found to be the strong candidates for the next generation of coolants for improving the design and performance of thermal management systems [2-4]. Researchers have been confused for the past five years with the anomalously high thermal conductivity of nanofluids. However, recently number of researchers proposed convection that is caused by the Brownian motion of nanoparticles to be one of the major physical mechanisms of the thermal conduction of nanofluids [5-7]. Therefore, it is important to examine the movements of nanoparticles in nanofluids. Stability of nanofluid is crucial and is quite essential to apply them for applications [8]. In the synthesis of nanofluids, agglomeration is a major problem. There are chiefly two techniques used to produce nanofluids: the single-step and the two-step method. In single step process, nanoparticles are simultaneously prepared and dispersed directly into the base fluid. This method avoids the processes of drying, storage, transportation, and dispersion of nanoparticles, so the agglomeration of nanoparticles is minimized and the stability of fluids is increased [9]. The drawback of the one step technique is that only low vapor pressure fluids are well-suited with such a process. The two-step method is largely used in the synthesis of nanofluids. In two-step process, nanoparticles are produced as a dry powder, and then dispersed into a fluid. But this method leads to agglomeration of nanoparticles and hence settlement. Therefore, the suspension prepared should be stabilized by some method. In general, these are effective methods used for preparation of stable suspensions: (1) using ultrasonic

vibration; (2) to change the PH value of suspensions; and (3) to use surface activators and/or dispersants [10]. Ultrasonication is a conventional technique for dispersing the highly aggregated nanoparticle samples for preparation of mixed aqueous nanosuspensions. Lee *et al.*, and Wang *et al.*, used this method to produce Al<sub>2</sub>O<sub>3</sub> nanofluids [11-12].

The study of intra and intermolecular interactions in the liquid system is very much essential and it gives information regarding the interacting properties of the molecules. Ultrasonic velocity is the speed in which sound propagates in a certain material. It depends on material density and elasticity. Although reports are available on the thermal conductivity and viscosity of nanofluids, very little work is reported on the acoustical properties of nanofluids [13-18]. M. Nabeel Rashin and J. Hemalatha have made ultrasonic investigations for stable cobalt ferrite nanofluids of various concentrations at different temperatures and magnetic fields [19]. They also studied the response of copper oxide - coconut oil nanofluids to the ultrasonic wave propagation [20]. Jay Kumar Patel and Kinnari Parekh studied ultrasound wave propagation in nanofluids and its rheological behavior as a function of temperature, volume fraction and magnetic field for magnetic nanofluids [21]. R. Kiruba *et al.*, reported ultrasonic studies of zinc oxide nanofluids [22]. Ultrasonic velocity measurements of the prepared nanofluids were carried out for six different concentrations at a fixed frequency of 2 MHz. Yadav *et al.*, studied ultrasonic attenuation and ultrasonic velocity in a polymer colloidal solution with dispersed nanoparticles [23]. They reported that the ultrasonic attenuation is directly proportional to the thermal conductivity of composites and the higher value of thermal conductivity of the nanofluids has an impressive effect on the total ultrasonic attenuation. Hence, this paper is focused on the systematic experimental study on the preparation of CuO nanofluids and to elucidate the interactions in the dispersed nanofluid matrix study using ultrasonic technique. CuO nanofluids are prepared using two-step method with ethylene glycol as base fluid. Ethylene glycol (EG) is often used due to its lower freezing point and can be useful in industrial fields as solvents, carriers, lubricants, binders, bases and coupling agents and also for extraction, separation, and purification of materials [24]. CuO nanoparticles are of particular interest because of their extensive use in catalysis, metallurgy, high temperature superconductors and as proficient nanofluid in heat transfer applications [25-27]. Copper oxide nanoparticles are industrially important material that has been used in applications such as gas sensors, [28] magnetic storage media, [29] solar energy transformation, [30] photovoltaic cells [31] and catalysis [32,33]. Recently, CuO nanoparticles have been used as an antimicrobial agent [34]. Also CuO nanoparticles are used in chemotherapy for patients with AIDS [35]. Ultrasonic wave technique is utilized and the effect of particle concentration and temperature on the ultrasonic velocity in CuO nanosuspensions in ethylene glycol (EG) is investigated. The acoustical parameters are calculated to analyze the interactions occurring in the nanofluid system and the results are discussed. The main aim of this study is to prepare the stable and homogeneous copper oxide nanofluids and to understand particle– fluid, particle–particle interactions as functions of concentration and temperature.

## EXPERIMENTAL SECTION

### a) Synthesis

The synthesis of copper oxide nanoparticles is carried out by precipitating copper salt in alkaline medium [36]. The copper salt used is freshly prepared 0.2 M CuCl<sub>2</sub>·H<sub>2</sub>O. The salt solution is mixed with 1ml glacial acetic acid and the resultant solution is heated to 80°C under magnetic stirring. Higher temperature is favored for higher reaction rates, which produces large amounts of nuclei to form in a short time, and the aggregation of crystals is inhibited. Glacial acetic acid is used to avoid the hydrolysis of the copper chloride solution. On vigorous stirring, the pH of above solution is increased rapidly to 12.5 by adding aqueous NaOH solution. The color of the solution turned from blue to black immediately, and a black suspension formed simultaneously. At the same pH, temperature and stirring speed, the solution is kept at a digestion time of 2 hours. Overall chemical reaction can be written as



The mixture was cooled to room temperature and centrifuged. The precipitates were washed with triply distilled water and absolute ethanol for several times and then dried at 60°C. After dried at 60°C, the precipitate was annealed at 400°C for 3h in ambient atmosphere to get black oxide product CuO.

Nanofluids of various nanoparticle concentrations (0.2%, 0.4%, 0.6%, 0.8%, and 1% by weight) in ethylene glycol were prepared by dispersing a specified amount of copper oxide nanoparticles in the base fluid, Fig. 1. Ultrasonication process is used to suppress the formation of particle clusters and to obtain stable suspensions. A

special thermostatic water bath arrangement was made for density, ultrasonic velocity and viscosity measurements, in which temperature variation was maintained within  $\pm 0.01^\circ\text{C}$ . The velocity values of ultrasonic wave propagation through the nanofluid samples were measured using a multi frequency ultrasonic interferometer (Model F81, Mittal Enterprises, New Delhi), with an accuracy of  $\pm 0.05\%$  at frequency of 6 MHz. An experimental set-up is shown in Fig. 2

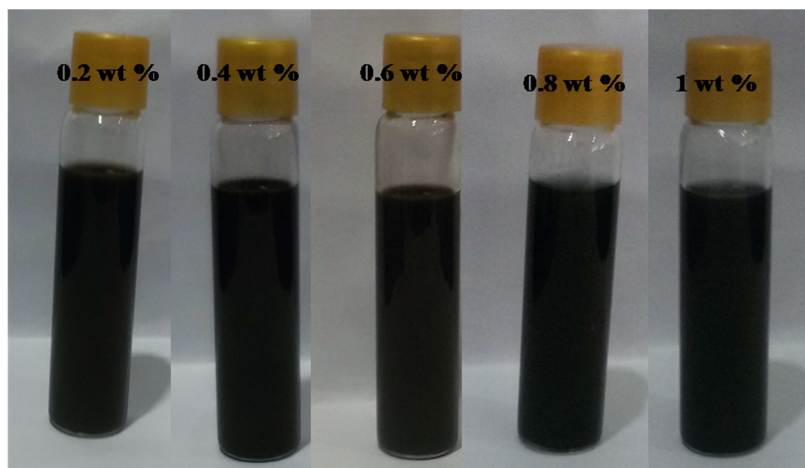


Fig. 1: Vials containing CuO NPs in Ethylene Glycol

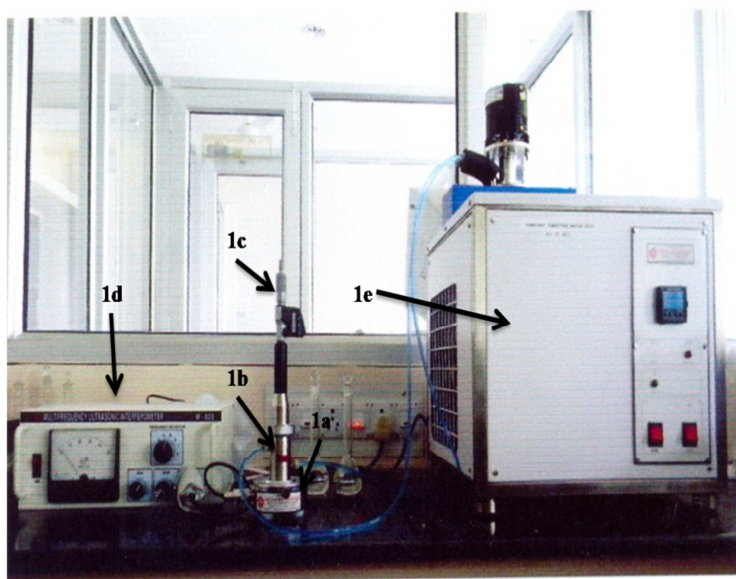


Fig. 2: Experimental set-up 1: (a) base to hold cell, (b) double jacketed measuring cell containing quartz crystal for generating 6 MHz frequency, (c) top part of the cell with micrometer screw gauge which moves reflector plate up and down and (d) multifrequency ultrasonic waves generator, (e) constant temperature bath

Density of the fluid was determined using specific gravity bottle (5 cc) with accuracy of  $\pm 2$  parts in  $10^4$ . Viscosity of the fluid was measured by Ostwald viscometer. The accuracy of viscosity in this method is  $\pm 0.001 \text{ Nsm}^{-2}$ . All these measurements were performed for the fluids of all concentrations at three different temperatures of 25, 30 and  $35^\circ\text{C}$ . The velocity and density measurements were repeated several times for accuracy and the average of the continuous consistent values are reported in this paper.

**b)Characterization**

The crystalline structure, phase composition and crystallite size of CuO were identified from XRD patterns obtained using Cu K $\alpha$  radiation ( $\lambda = 1.541 \text{ \AA}$ ) for  $2\theta$  value ranging from  $10^\circ$  to  $60^\circ$  in X-ray diffractometer (Bruker AXS D8 Advance). The UV-visible absorption spectrum was recorded using Lambda 750 Perkin Elmer UV-VIS-NIR Spectrophotometer for optical characterization. The size and morphology of nanoparticle is found using Transmission Electron Microscope (Hitachi (H-7500) microscope) operating at 80 kV. Powder Sample for TEM measurements is suspended in ethanol and ultrasonically dispersed. Drops of the suspensions are placed on a copper grid coated with carbon. The morphology of the particles is observed by a scanning electron microscope (SEM-EDS) using SEM make JEOL Model JSM - 6390LV and EDS make JEOL Model JED – 2300 with an accelerating voltage of 20 kV.

**RESULTS AND DISCUSSION****a)Structural Studies**

Figure 3 shows the XRD pattern of CuO nanoparticles. The XRD diffractogram of CuO nanopowder consists of diffractions peaks at  $32.7^\circ$ ,  $35.7^\circ$ ,  $39.0^\circ$ ,  $48.9^\circ$ ,  $53.7^\circ$ ,  $58.5^\circ$ , correspond to (110), (002), (111), (202), (020) and (113) reflections of CuO [37]. All the peaks can be indexed to the monoclinic crystal system CuO. The crystallite size has been estimated from the XRD pattern using the Scherrer's equation [38].

$$D = K\lambda / \beta \cos\theta \quad (1)$$

where K is a constant (0.9);  $\lambda$  is the X-ray wavelength used in XRD (0.154 nm);  $\theta$  is the Bragg angle;  $\beta$  is the FWHM (full width at half maximum intensity), that is, broadening due to the crystallite dimensions. The average crystallite size of CuO nanoparticles is found to be around 18.48 nm.

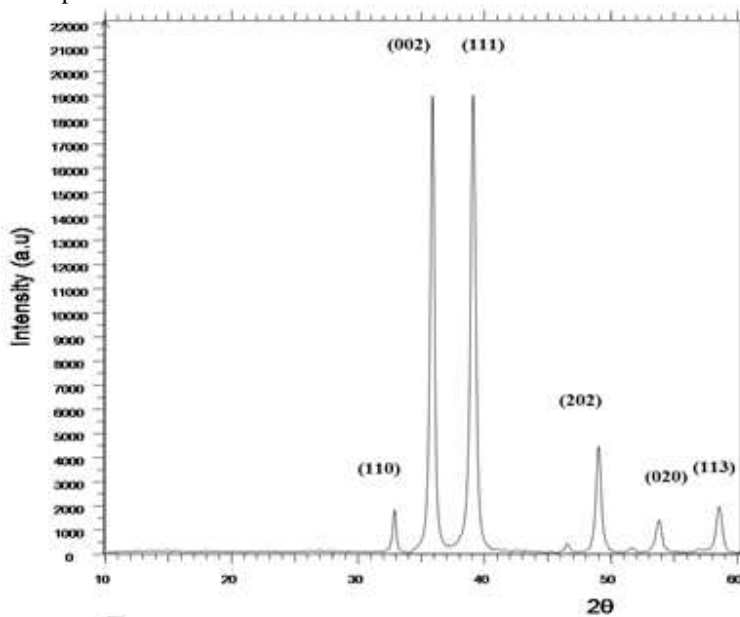


Fig 3: XRD spectra of CuO nanoparticles

Fig. 4(a) shows the wavelength versus absorption plot. CuO nanoparticles showed a band at  $\sim 280 \text{ nm}$  due to metal inter band transitions and a broad absorption peak between  $450$  and  $550 \text{ nm}$  can be contributed to the characteristic absorption of CuO NPs [39,40]. In order to calculate the optical band gap of sample Tauc's relation in the following equation is used [41]:

$$(Ah\nu)^n = B(h\nu - E_g) \quad (2)$$

in which  $h\nu$  is photo energy,  $A$  is absorption coefficient,  $B$  is a material constant,  $E_g$  is band gap. The band gap can be estimated by extrapolating the linear region in the plot of  $(Ah\nu)^2$  versus photon energy as shown in the Fig. 4(b). The band gap of nano CuO is calculated to be 3.47 eV, which is higher than the reported value of CuO in the range from 1.8-2.5 eV [42]. The increase in band gap may be due to the quantum size effect of the synthesized sample [43].

Figure 5 shows the structural morphology (TEM) of the CuO nanostructures. The particle size observed in TEM image is in the range of 9-18 nm which is in good agreement with the calculated results by Scherrer formula. Fig. 6 shows the SEM micrograph of the CuO nanoparticles at 15,000X magnification. The SEM micrograph indicates needle shape for CuO nanoparticles. The SEM micrographs revealed little aggregates of chemically synthesized nanoparticles. EDS spectrum of CuO nanoparticles is given in Fig. 7. The EDS result shows that there are no other elemental impurities present in the prepared CuO nanoparticles.

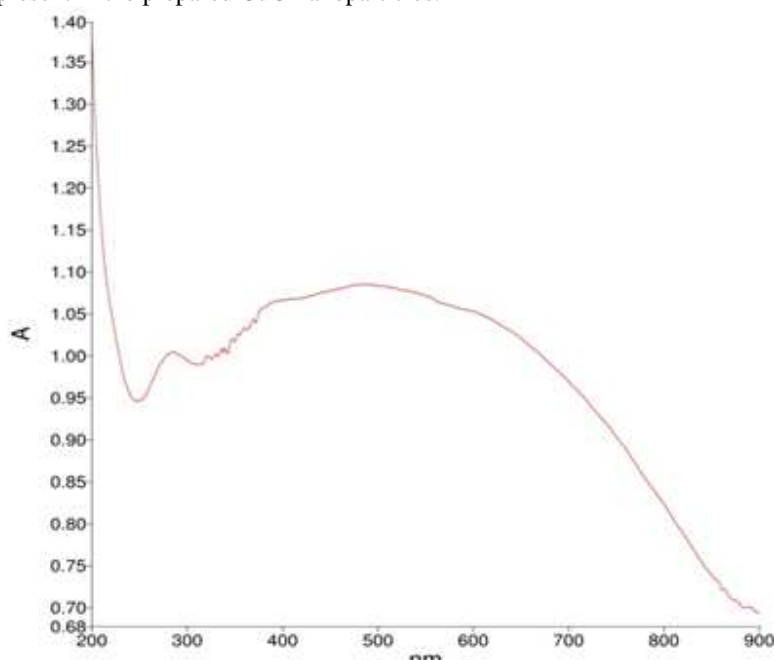


Fig 4a: UV-Vis spectra of CuO nanoparticles

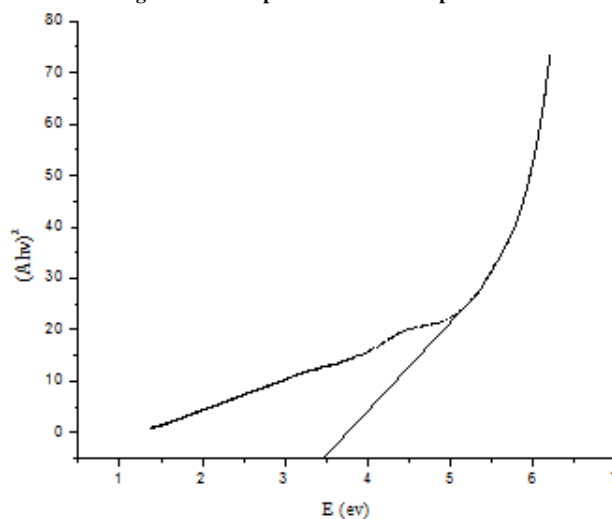


Fig. 4b: Plot of  $(Ah\nu)^2$  versus  $E$  (eV)

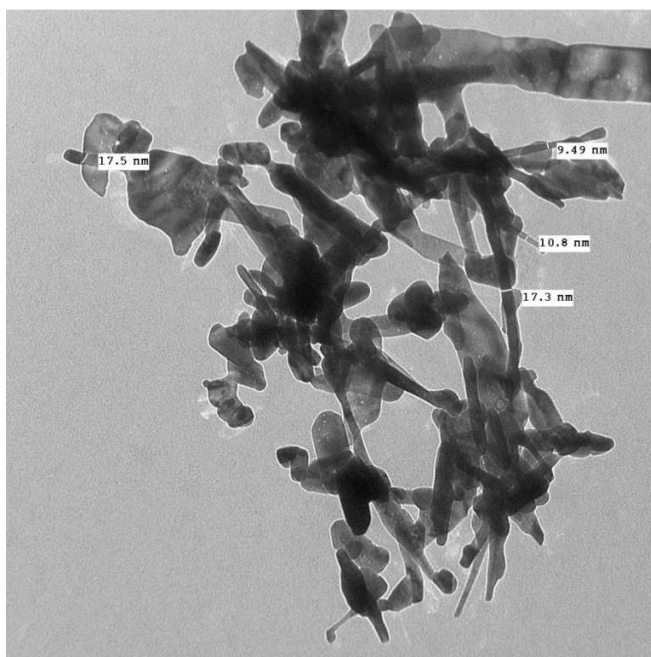


Fig 5: TEM micrograph of CuO nanoparticles

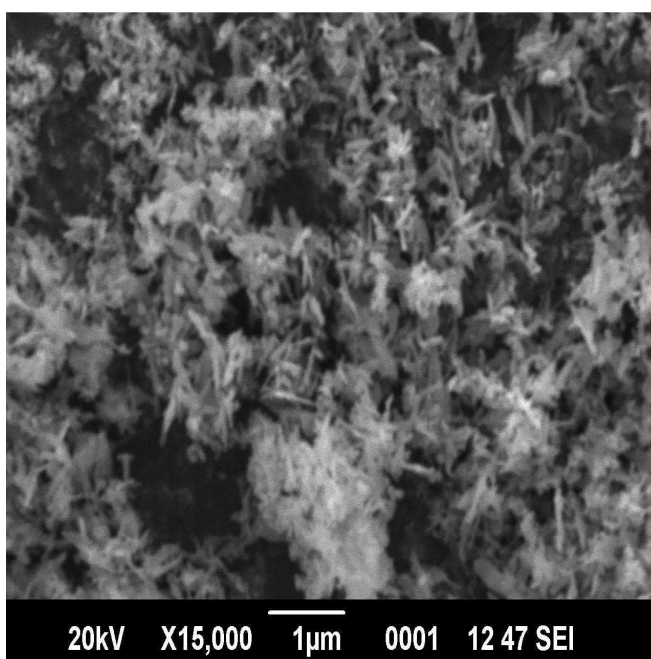


Fig 6: SEM micrograph of CuO nanoparticles

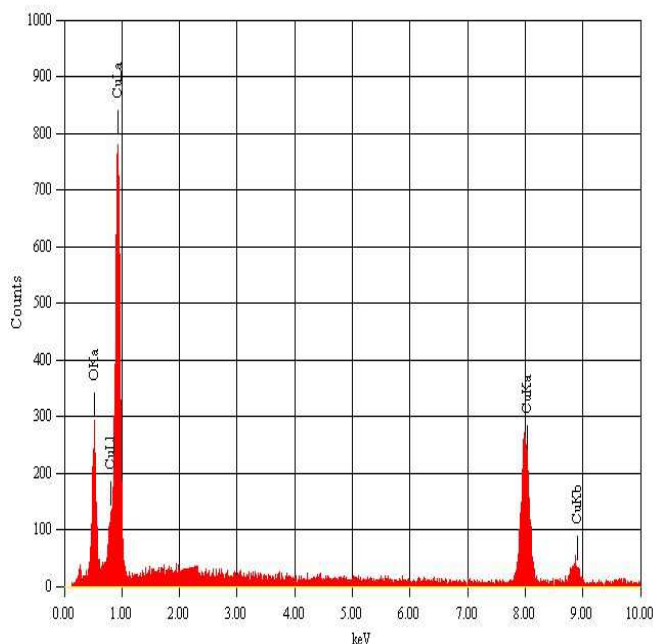


Fig 7: EDS of CuO nanoparticles

**b) Ultrasonic studies**

The velocity of ultrasonic waves in the liquid can be obtained by the relation;

$$U = \lambda \times f \quad \text{ms}^{-1} \quad (3)$$

where  $f$  is the frequency of the generator and  $\lambda$  is the wavelength of ultrasonic waves in the liquid. The acoustical parameters [44] like adiabatic compressibility ( $\beta_{ad}$ ), intermolecular free length ( $L_f$ ), relaxation time ( $\tau$ ), absorption coefficient ( $a/f^2$ ), acoustic impedance ( $Z$ ), Gibb's free energy ( $\Delta G$ ), free volume ( $V_f$ ), rao's constant ( $R_M$ ) and wada's constant ( $W$ ), were measured for prepared nanofluids using velocity, density and viscosity data obtained through the experimental data. By using ultrasonic velocity data, adiabatic compressibility was calculated by using the Newton-Laplace's equation [45],

$$\beta_{ad} = 1/U^2 \rho \quad (\text{N}^{-1}\text{m}^2) \quad (4)$$

Where,  $u$  is velocity &  $\rho$  is density of nanofluid.

Intermolecular free length is determined using the following formula given by Jacobson [46],

$$L_f = K_T \beta_{ad}^{1/2} \quad (\text{m}) \quad (5)$$

where,  $K_T$  is Jacobson's constant. This constant is a temperature dependent parameter whose value at 25, 30 and 35°C is  $2.0568 \times 10^{-6}$ ,  $2.0756 \times 10^{-6}$  and  $2.0943 \times 10^{-6}$  respectively.

The relaxation time can be calculated from the relation [47],

$$\tau = (4/3)\beta\eta \quad (\text{s}) \quad (6)$$

Absorption coefficient can be calculated using the relation,

$$(a/f^2) = 4\pi^2\tau/2U \quad (\text{s}^2\text{m}^{-1}) \quad (7)$$

Acoustic impedance is determined from equation [48],

$$Z = U \times \rho \quad (\text{Nsm}^{-3}) \quad (8)$$

Gibbs free energy is calculated from acoustic relaxation time ( $\tau$ ) as follows,

$$\Delta G = kT \ln \left( \frac{kT\tau}{h} \right) \quad (\text{Jmol}^{-1}) \quad (9)$$

Free volume is calculated by following equation obtained on the basis of dimension analysis by [49],

$$V_f = \left( \frac{M_{\text{eff}}U}{K\eta} \right)^{3/2} \quad (\text{m}^3\text{mol}^{-1}) \quad (10)$$

where  $M_{\text{eff}}$  is the effective molecular weight, which is expressed as  $M_{\text{eff}} = \Sigma M = m_i x_i$  where,  $x$  and  $m$  are the mole fraction and molecular weight of the individual component in the mixture respectively.  $K$  is the temperature independent constant and its value is  $4.28 \times 10^9$ .

Molar compressibility or Wada's constant is calculated by following equation,

$$W = \left( \frac{M_{\text{eff}}}{\rho} \right) \beta_{\text{ad}}^{-1/7} \quad (\text{m}^3/\text{mole}(\text{N/m}^2)^{1/7}) \quad (11)$$

Molar sound speed or Rao's constant is calculated by using following equation,

$$R_M = \left( \frac{M_{\text{eff}}}{\rho} \right) U^{1/3} \quad (\text{m}^{10/3}\text{s}^{-1/3}\text{mol}^{-1}) \quad (12)$$

The parameters like ultrasonic velocity, density and viscosity of nanofluids of various concentrations are listed in Table 1, adiabatic compressibility, intermolecular free length, and relaxation time are listed in Table 2, absorption coefficient, acoustic impedance and Gibb's free energy are tabulated in Table 3 and free volume, rao's constant and wada's constant are listed in Table 4.

### Effect of concentration

The ultrasonic velocities measured for pure ethylene glycol and prepared nanofluids at three different temperatures are shown in Fig. 8(a). The velocity curves indicate that the ultrasonic velocity in the samples increases to a maximum value up to 0.6 wt % above which it starts decreasing at a temperature of 25°C. It shows the influence of dispersed particles on the velocity of ultrasonic propagation. This may be possibly due to more surface area of nanoparticles due to which more ethylene glycol molecules can be adsorbed on its surface. So they can move from one point to another point easily. Also, the interaction between nanosized copper oxide particles and microsized ethylene glycol molecules through secondary forces of interaction leads to the formation of hierarchical structure and hence enhancement of velocity. This clearly indicates that there is strong particle-fluid interaction favoring increase in velocity up to 0.6 wt % [22]. The random movements of nanoparticles are increased with increase in concentration and when the ultrasonic vibration is propagated in nanofluid, Brownian motion stops the fluid particles in suspension, leading to decrease in velocity. Therefore above this concentration, the velocity in nanofluid decreases. This indicates that there is decrease in the nanoparticle-fluid interaction and particle-particle interaction becomes predominant leading to decrease in velocity value.

From table 1, it is evident that viscosity first decreases upto critical concentration, 0.6 wt % and then increases with increasing nanoparticle loading. Decrease in viscosity may be due to small disturbances in hydrogen bonding network of strongly-hydrogen bonded liquids and ethylene glycol is one of them with extensive hydrogen bonding network [50, 51]. The dispersion of CuO nanoparticles in ethylene glycol might perturb the hydrogen bonding between ethylene glycol molecules, due to interaction between nanoparticles and ethylene glycol molecules. With increasing nanoparticle concentration, the number of CuO nanoparticles interacting with ethylene glycol molecules becomes higher and hence, disturbances to the hydrogen bonding network of ethylene glycol were increased leading to reduction in viscosity [52] in the range of 0–0.6 wt%. But beyond 0.6 wt % nanoparticle loading, agglomeration leads to decrease in particle-fluid interaction and hence increase in viscosity. Above this critical concentration of 0.6 wt%, the viscosity reduction due to perturbation of hydrogen bond between ethylene glycol molecules is prevailed over by viscosity increase due to addition of CuO nanoparticles. Hence, it may be conclude that viscosity of CuO-ethylene glycol nanofluid is determined by the relationship between perturbation of hydrogen bonding network and increased viscous dissipation due to nanoparticles' addition.

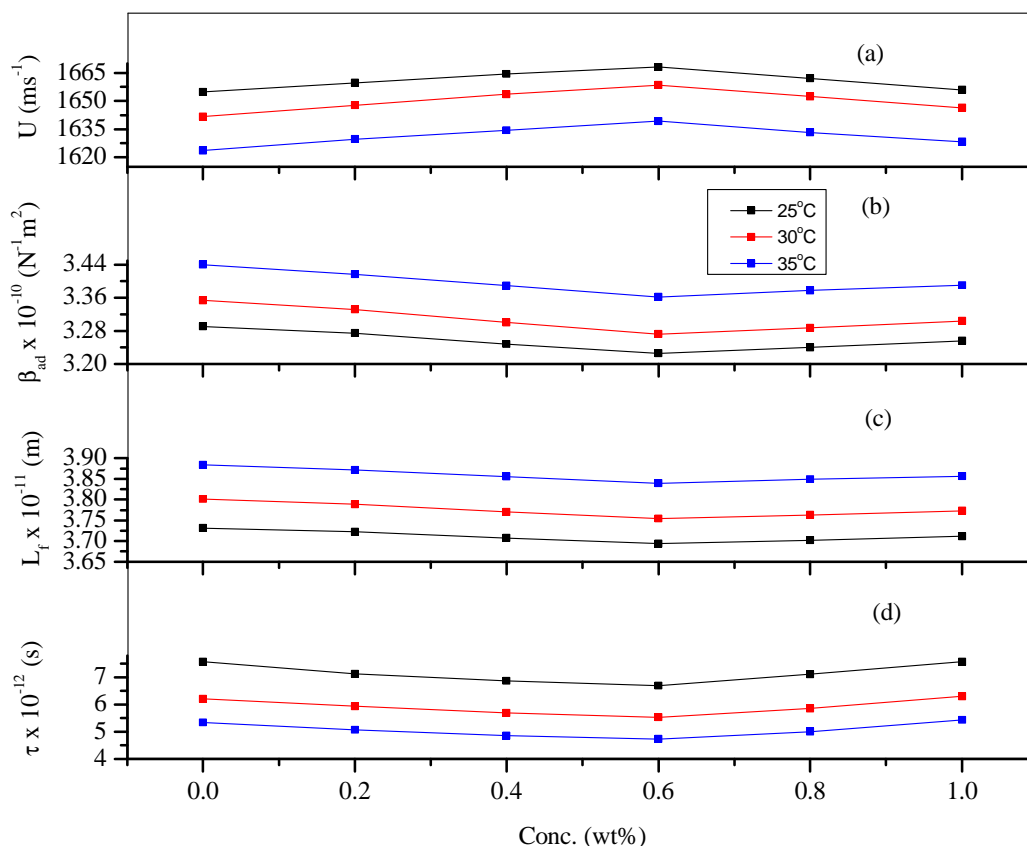


Fig 8: Plots of a) Ultrasonic velocity versus concentration b) adiabatic compressibility versus concentration and c) intermolecular free length versus concentration d) relaxation time versus concentration for nanofluids at various temperatures

Table 1: Velocity, density and viscosity of CuO nanofluids at 25, 30 and 35°C

Temp (°C)	Conc. (wt%)	U (ms <sup>-1</sup> )	$\rho \times 10^3$ (Kg m <sup>-3</sup> )	$\eta \times 10^{-3}$ (Nsm <sup>-2</sup> )
25	0	1654.8	1.1098	17.25*
	0.2	1659.6	1.1087	16.3298
	0.4	1664.4	1.1115	15.8618
	0.6	1668	1.1143	15.5569
	0.8	1662	1.1175	16.4519
	1	1656	1.1200	17.4258
30	0	1641.6	1.1063	13.86*
	0.2	1647.6	1.1056	13.3422
	0.4	1653.6	1.1082	12.9217
	0.6	1658.4	1.1113	12.6846
	0.8	1652.4	1.1141	13.3525
	1	1646.4	1.1166	14.2909
35	0	1623.6	1.1028	11.64*
	0.2	1629.6	1.1021	11.1268
	0.4	1634.4	1.1046	10.7491
	0.6	1639.2	1.1071	10.5475
	0.8	1633.2	1.1100	11.0923
	1	1628.4	1.1124	12.0058

Note: \* Literature value [53]

The value of adiabatic compressibility and intermolecular free length shows an opposite behavior as compared to the ultrasonic velocity. The values of compressibility (Fig. 8(b)), and intermolecular free length (Fig. 8(c)) are found to

first decrease upto 0.6 wt% above which it starts increasing with increase in particle concentration. The decrease in adiabatic compressibility and free length indicates a significant interaction between particles and base fluid molecules [54]. In general  $U$  and  $L_f$  have been reported to vary inversely of each other with the composition of the mixture as in the present system [55]. It is evident from Fig. 8(d) that relaxation time first decreases and then increases with increase in concentration of solution. The relaxation time which is in the order of  $10^{-12}$  sec is due to structural relaxation process [56] and in such a situation it is suggested that the molecules get rearranged due to co-operative process [57]. It is observed that at 0.6 wt %, there is increase in absorption coefficient which suggests that there may be weak interactions between particles and base fluid molecules. Below this critical concentration, absorption coefficient decreases. Such decreasing trends further support the possibility of strong interaction between particles and fluid molecules [17].

**Table 2: Adiabatic compressibility, intermolecular free length and relaxation time of CuO nanofluids at 25, 30 and 35°C**

Temp	Conc. (wt%)	$\beta_{ad} \times 10^{10}$ ( $N^{-1}m^3$ )	$L_f \times 10^{-11}$ (m)	$\tau \times 10^{-12}$ (s)
25	0	3.2905	3.7310	7.5682
	0.2	3.2748	3.7220	7.1302
	0.4	3.2477	3.7066	6.8686
	0.6	3.2256	3.6940	6.6906
	0.8	3.2396	3.7020	7.1063
	1	3.2558	3.7113	7.5647
30	0	3.3542	3.8014	6.1986
	0.2	3.3320	3.7887	5.9274
	0.4	3.3001	3.7705	5.6856
	0.6	3.2718	3.7544	5.5336
	0.8	3.2874	3.7633	5.8526
	1	3.3039	3.7728	6.2955
35	0	3.4399	3.8843	5.3387
	0.2	3.4168	3.8712	5.0690
	0.4	3.3891	3.8555	4.8572
	0.6	3.3616	3.8398	4.7276
	0.8	3.3775	3.8489	4.9953
	1	3.3901	3.8561	5.4268

**Table 3: Absorption coefficient, acoustic impedance and Gibb's free energy of CuO nanofluids at 25, 30 and 35°C**

Temp	Conc. (wt%)	$\alpha/f^2 \times 10^{-14}$ ( $s^2m^{-1}$ )	$Z \times 10^6$ ( $Nsm^{-3}$ )	$\Delta G \times 10^{-21}$ ( $Jmol^{-1}$ )
25	0	9.0185	1.8365	15.8437
	0.2	8.4720	1.8400	15.5984
	0.4	8.1376	1.8500	15.4446
	0.6	7.9097	1.8587	15.3365
	0.8	8.4315	1.8573	15.5846
	1	9.0079	1.8547	15.8418
30	0	7.4459	1.8161	15.3437
	0.2	7.0942	1.8216	15.1565
	0.4	6.7801	1.8325	14.9822
	0.6	6.5797	1.8430	14.8688
	0.8	6.9843	1.8409	15.1034
	1	7.5402	1.8384	15.4086
35	0	6.4840	1.7905	15.0312
	0.2	6.1339	1.7960	14.8107
	0.4	5.8603	1.8054	14.6292
	0.6	5.6872	1.8148	14.5141
	0.8	6.0313	1.8129	14.7484
	1	6.5717	1.8114	15.1008

From Fig. 9(b), it is found that there is an increase in acoustic impedance values with increase in concentration of particles and then it decreases with further increase in concentration. It implies that the  $Z$ -values show similar behavior to that of ultrasonic velocity values [54, 55]. Specific acoustic impedance is defined as the resistance offered to the sound wave by the components of the mixture. It is almost reciprocal of adiabatic compressibility. The decrease of  $Z$  value at 0.6 wt % concentration shows weak interactions similar to ultrasonic velocity. The higher values of acoustic impedance indicate that there is a significant interaction between the particle and base fluid molecules. Gibbs free energy confirms the same (relaxation time) from the measured values that are given in the

Table 3. The plot of free volume versus concentration reveals that the values first increase and after 0.6 wt % it goes on decreasing. The increase in free volume with concentration is indicating the association through hydrogen bonding [58]. It shows the increasing magnitude of interaction between CuO nanoparticles and ethylene glycol molecules. But as particle-fluid interaction decreases after 0.6 wt%, hence free volume decreases showing particle-particle interaction predominance.

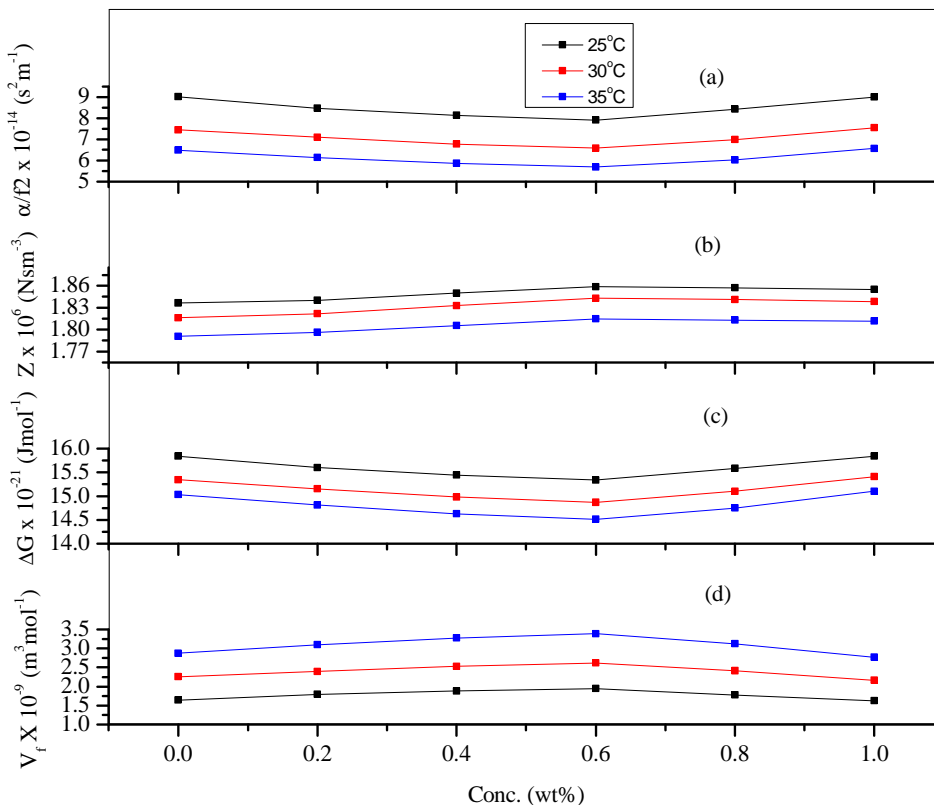


**Fig. 9:** Plots of a) Absorption coefficient versus concentration b) acoustic impedance versus concentration c) Gibb’s free energy versus concentration d) free volume versus concentration for nanofluids at various temperatures

**Table 4:** Free volume, wada’s constant and rao’s constant of CuO nanofluids at 25, 30 and 35°C

Temp	Conc. (wt%)	$V_f \times 10^{-9}$ ( $m^3 mol^{-1}$ )	$W \times 10^{-3}$ $m^3 mol^{-1} (Nm^{-2})^{1/7}$	$R_M \times 10^{-4}$ ( $m^{10/3} s^{-1/3} mol^{-1}$ )
25	0	1.6409	1.2657	6.6154
	0.2	1.7904	1.2683	6.6310
	0.4	1.8798	1.2672	6.6239
	0.6	1.9428	1.2658	6.6148
	0.8	1.7780	1.2620	6.5909
	1	1.6233	1.2588	6.5711
30	0	2.2512	1.2662	6.6186
	0.2	2.3980	1.2687	6.6335
	0.4	2.5317	1.2681	6.6293
	0.6	2.6160	1.2666	6.6200
	0.8	2.4107	1.2632	6.5983
	1	2.1667	1.2600	6.5783
35	0	2.8770	1.2656	6.6152
	0.2	3.0973	1.2682	6.6302
	0.4	3.2789	1.2674	6.6250
	0.6	3.3903	1.2665	6.6193
	0.8	3.1285	1.2630	6.5969
	1	2.7678	1.2601	6.5790

Molar sound velocity i.e. rao's constant shows a nonlinear variation with concentration of particles [59]. The trends of variation of wada's constant with concentration are reported in Table 4 and are in accordance with the observed variation of rao's constant with concentration. This increasing trend of rao's constant and wada's constant upto 0.6 wt % indicates that availability of more number of components in a given region of space [60].

### Effect of temperature

The plots of velocity versus concentration obtained at 30 and 35 °C have the same trend as the plot obtained at 25 °C, but with lower magnitudes of velocity. With the increase of temperature, there was rapid movement of suspended molecules in the liquid matrix and hence it enhances the compressibility (Fig. 8(b)) and hence decreases velocity (Fig. 8(a)). This proves that at high temperatures there is weakening of the particle–fluid interaction. There is uniform decrease in density with increase in temperature which reveals the weakening of intermolecular forces due to thermal agitation of the molecules. Viscosity also decreases with increase in temperature which reveals the weakening of intermolecular forces due to thermal agitation of the molecules as there is increase in thermal energy of the system. The decrease in viscosity of liquids with increasing temperatures is due to decrease in the extent of intermolecular attractive forces such as hydrogen bonds [61]. With reduction in intermolecular forces of attraction at higher temperatures, their influence on viscosity is also reduced. This causes an increase in volume and hence decreases in density and viscosity [62]. Intermolecular free length increases linearly with temperature as shown in Fig. 8(c) [63,64]. As the temperature increases it leads to the less ordered structure and more spacing between the molecules due to increase in thermal energy of the system which results in volume expansion and hence increase in inter molecular free length. Absorption coefficient, acoustic impedance and Gibb's free energy decreases with temperature whereas free volume increases with temperature as presented in Fig. 9(a), 9(b), 9(c) and 9(d). Same trend of absorption coefficient were reported earlier by Naik *et al.*, and Umadevi and Kesavasamy [58, 65]. Decrease of acoustic impedance with temperature shows weakening of interactions similar to ultrasonic velocity. Increase in free volume shows enhancement in disorder in the liquid because of increased mobility of the molecules [66]. Same trends were reported earlier [67]. Relaxation time is observed to decrease with temperature, Fig 8(d). With increase in temperature excitation energy increases and hence relaxation time decreases [65]. Further as the kinetic energy of the molecule increases, it takes long time for rearrangement of molecule and this suggests a decrease in Gibb's free energy, Fig. 9(c). Rao's constant as well as wada's constant both increases with temperature [58]. These trends are in accordance with ultrasonic velocity and density data.

### CONCLUSION

The ultrasonic velocity, density and viscosity in CuO nanofluid has been investigated for different concentration of particles in ethylene glycol based fluid at temperatures 25, 30 and 35 °C. Various acoustical parameters were evaluated using the experimental data. Interaction between particles and ethylene glycol molecules was analyzed using acoustical parameters. The increase in ultrasonic velocity with increase in concentration can be explained using increase in particle–fluid interaction up to a critical concentration of 0.6 wt % above which the particle–fluid interaction weakens due to strong particle–particle interaction. From the analysis of all acoustical parameters, it is evident that particle – particle interaction becomes predominant after 0.6 wt % due to agglomeration. But at higher temperatures, ultrasonic velocity decreases because of decrement in particle-fluid interaction. It is observed that there is particle–fluid interaction which favors increase in velocity. Such particle–fluid interaction studies are helpful to understand the reasons behind unusual enhancements in physical properties of nanofluids and to comprehend the mechanism of fluid flow in nanoscale. It may be concluded that ultrasonic velocity is higher for nanofluids compared with base liquid for better enhancement of nanosuspension that could be used for industrial applications. So we may conclude that the concentration of nanofluid upto 0.6 % in which nanoparticle-fluid interaction is significant and is highly suitable for nanofluid applications.

### Acknowledgements

The authors are thankful to Department of Chemistry (University of Jammu) for providing necessary facilities and support for conducting present study and CSIR UGC for Junior Research Fellowship (JRF) to the first author. The authors gratefully acknowledge SAIF STIC (Kochi), SAIF Chandigarh, CIL Chandigarh for providing the facilities for characterization.

### REFERENCES

- [1] SUS Choi, in: *Proceedings of the American Society of Mechanical Engineers (ASME)*, New York, **1995**, 66, 99.

- [2] JA Eastman; SUS Choi; S Li; W Yu; LJ Thompson, *Appl. Phys. Lett.*, **2001**, 78, 718.
- [3] SUS Choi; ZG Zhang; W Yu; FE Lockwood; EA Grulke, *Appl. Phys. Lett.*, **2001**, 79, 2252.
- [4] DH Kumar; HE Patel; VRR Kumar; T Sundarajan; T Pradeep; SK Das, *Phys. Rev. Lett.*, **2004**, 93, 144301.
- [5] J Koo; C Kleinstreuer, *J. Nanopart. Res.*, **2004**, 6, 577.
- [6] R Prasher; P Bhattacharya; PE Phelan, *J. Heat Trans.*, **2006**, 128, 588.
- [7] Y Xuan; Q Li, *J. Appl. Phys.*, **2006**, 100, 043507.
- [8] Y Wei; X Huaqing; C Lifei; L Yang, *Powder Technol.*, **2010**, 197, 218.
- [9] Y Li; J Zhou; S Tung; E Schneider; S Xi, *Powder Technol.*, **2009**, 196, 89.
- [10] Y Xuan; Q Li, *Int. J. Heat Fluid Flow*, **2000**, 21, 58.
- [11] S Lee; SUS Choi; S Li; JA Eastman, *J. Heat Trans.*, **1999**, 121, 280.
- [12] X Wang; X Xu; SUS Choi, *J. Thermophys. Heat Trans.*, **1999**, 13, 474.
- [13] DK Singh; DK Pandey; RR Yadav, *Ultrasonics*, **2009**, 49, 634.
- [14] T Hornowski; A Józefczak; M Łabowski; A Skumiel, *Ultrasonics*, **2008**, 48, 594.
- [15] P Sayan; J Ulrich, *Chem. Eng. Process*, **2002**, 41, 281.
- [16] M Motozawa; Y Iizuka; T Sawada, *J. Phys. Condens. Matter.*, **2008**, 20, 204117-1.
- [17] J Hemalatha; T Prabhakaran; RP Nalini, *Microfluid. Nanofluid.*, **2011**, 10, 263.
- [18] R Kiruba; AKS Jeevaraj, *Integrated Ferroelectrics*, **2014**, 150, 59.
- [19] MN Rashin; J Hemalatha, *Ultrasonics*, **2014**, 54, 834.
- [20] MN Rashin; J Hemalatha, *Int. J. Eng. Appl. Sci.*, **2012**, 6, 216.
- [21] JK Patel; K Parekh, *Ultrasonics*, **2015**, 55, 26.
- [22] R Kiruba; M Gopalakrishnan; T Mahalingam; AKS Jeevaraj, *J. Nanofluids*, **2012**, 1, 97.
- [23] RR Yadav; G Mishra; PK Yadava; SK Kor; AK Gupta; B Raj; T Jayakumar, *Ultrasonics*, **2008**, 48, 591.
- [24] M Taghi; Z Moattar; RM Cegincara, *J. Chem. Thermodyn.*, **2012**, 54, 55.
- [25] PO Larsson; A Andersson, *J. Catal.*, **1998**, 179, 72.
- [26] V Chikán; Á Molnár; K Balázsik, *J. Catal.*, **1999**, 184, 134.
- [27] CP Poole, T Datta, HA Farach, MM Rigney, CR Sanders. *Copper Oxide Superconductors*, John Wiley & Sons, New York, **1988**.
- [28] ML Zhong; DC Zeng; ZW Liu; HY Yu; XC Zhong; WQ Qiu, *Acta Mater.*, **2010**, 58, 5926.
- [29] P Dai; HA Mook; G Aepli; SM Hayden; F Dogan, *Nature Mater.*, **2000**, 406, 965.
- [30] S Anandan; X Wen; S Yang, *Mater. Chem. Phys.*, **2005**, 93, 35.
- [31] KL Hardee; AJ Bard, *J. Electrochem. Soc.*, **1977**, 124, 215.
- [32] JB Reitz; EI Solomon, *J. Am. Chem. Soc.*, **1998**, 120, 11467.
- [33] F Teng; W Yao; Y Zheng; Y Ma; Y Teng; T Xu; S Liang; Y Zhu, *Sensors and Actuators B*, **2008**, 134, 761.
- [34] G Ren; D Hu; EWC; Cheng; MAV Reus; P Reip; RP Allaker, *Int. J. Antimicrob. Agents*, **2009**, 33, 587.
- [35] N Krithiga; A Jayachitra; A Rajalakshmi, *Indian J. Nanosci.*, **2013**, 1, 6.
- [36] NR Karthikeyan; J Philip; B, Raj, *Mater. Chem. Phys.*, **2008**, 109, 50.
- [37] MA Siddiqui; HA Alhadlaq; J Ahmad; AA Al-Khedhairy; J Musarrat; M Ahamed, *PLOS ONE*, **2013**, 8, e69534.
- [38] AL Patterson, *Phys. Rev.*, **1939**, 56, 978.
- [39] M Rashad; M Rüsing; G Berth; K Lischka; A Pawlis, *J. Nanomater.*, **2013**, 2013, Article ID 714853, 6 pages.
- [40] Rajgovind; G Sharma; D Gupta Kr; ND Jasuja; SC Joshi, *J. Microb. Biochem. Technol.*, **2015**, 7, 140.
- [41] J Tauc, *Mater. Res. Bull.*, **1968**, 3, 37.
- [42] N Wang; H He; L Han, *Appl. Surface Sci.*, **2010**, 256, 7335.
- [43] A Gulino; P Dapporto; P Rossi; I Fragala, *Chem. Mater.*, **2003**, 15, 3748.
- [44] S Thirumarani; S Sudha, *J. Chem. Pharm. Res.*, **2010**, 2, 327.
- [45] JS Rowlinson, FL Swinton. *Liquid and liquid mixtures*, 3<sup>rd</sup> Edition, Butterworths, London, **1982**, 16.
- [46] B Jacobson, *Acta Chemica Scand.*, **1951**, 5, 1214.
- [47] JH Hildebrand, *J. Chem. Phys.*, **1959**, 31C, 1423.
- [48] L Prigogine, V Malhot. *The molecular theory of the solution*, North Holl Pub, Amster Dam, **1957**.
- [49] CV Suryanarayana; J Kuppasamy, *J. Acoust. Soc. Ind.*, **1976**, 4, 75.
- [50] Y Tan; Y Song; Q Zheng, *Nanoscale*, **2012**, 4, 6997.
- [51] M Chaplin, *Cond. Mat.*, **2007**, 0706, 1355.
- [52] KS Suganthi; VL Vinodhan; KS Rajan, *Appl. Energy*, **2014**, 135, 548.
- [53] MJ Pastoriza-Gallego; L Lugo; JL Legido; MM Piñeiro, *Nanoscale Res. Lett.*, **2011**, 6, 221.
- [54] V Gupta; AK Sharma; M Sharma, *J. Chem. Pharm. Res.*, **2014**, 6, 714.
- [55] V Gupta; AK Sharma; M Sharma, *Chem. Sci. Trans.*, **2014**, 3, 736.

- [56] LE Kinsler, AR Rray. Fundamentals of Acoustics, Wiley Eastern, New Delhi, **1989**.
- [57] A Ali; S Hyder; AK Nain, *Indian J. Phys.*, **2000**, 74 B, 63.
- [58] RR Naik; SV Bawankar; VM Ghodki, *J. Polymer and Biopolymer Phys. Chem.*, **2015**, 3, 1.
- [59] R Natarajan; P Ramesh, *J. Pure Appl. Indian Phys.*, **2011**, 1, 252.
- [60] N Santhi; J Madhumitha, *Int. J. Adv. Chem.*, **2014**, 2, 12.
- [61] MN Rashin; J Hemalatha, *Exp. Therm. Fluid Sci.*, **2013**, 48, 67.
- [62] MK Praharaj; P Mishra; S Mishra; A Satapathy, *J. Chem. Pharm. Res.*, **2013**, 5, 49.
- [63] MK Praharaj; P Mishra; S Mishra; A Satapathy, *Adv. Appl. Sci. Res.*, **2012**, 3, 1518.
- [64] S Panda; AP Mahapatra, *J. Chem. Pharm. Res.*, **2014**, 6, 818.
- [65] M Umadevi; R Kesavasamy, *Int. J. Res. Chem. Environ.*, **2012**, 2, 157.
- [66] P Chimankar Omprakash; R Shriwas; A Tabhane Vilas, *J. Chem. Pharm. Res.*, **2011**, 3, 587.
- [67] M Umadevi; R Kesavasamy, *Int. J. Chem. Environ. Pharm. Res.*, **2012**, 3, 72.